inhibited the glutamate-induced increase of NF-κB activity in a concentration-dependent manner (Fig. 3), with calculated EC_{50} values of 1.3 and 6 mM for ASA and NaSal, respectively. Parallel experiments in which cell viability was measured 24 hours later revealed a strict correlation between neuroprotective concentrations of anti-inflammatory drugs and blockade of NF-κB induction (EC_{50} values of 1.5 mM for ASA and 5.8 mM for NaSal). The salicylate effect on NF-κB/Rel proteins was specific. In fact, ASA and NaSal failed to modify the glutamate-mediated nuclear induction of the transcriptional complex AP-1 (Fig. 3).

Thus, at concentrations compatible with amounts in plasma during treatment of chronic inflammatory states, salicylates prevented glutamate-induced neurotoxicity. The neuroprotective effect correlated neither with the anti-inflammatory properties of these compounds nor with cyclooxygenase inhibition. In fact, indomethacin exerted anti-inflammatory but not neuroprotective properties, and NaSal was neuroprotective but did not interfere with cyclooxygenase activity (*3*). The common molecular target for ASA and NaSal but not for indomethacin (*10*, *16*) was the blockade of NF-κB induction, suggesting a link between neuroprotection and the nuclear event.

Here we provide evidence for an unusual pharmacological effect of ASA and its metabolite NaSal. In view of their distinct ability to act not merely as anti-inflammatory compounds but also as neuroprotective agents against excitotoxicity, these drugs appear to possess a wider pharmacological spectrum than other nonsteroidal anti-inflammatory drugs.

REFERENCES AND NOTES

1. S. A. Lipton and P. A. Rosenberg, *N. Engl. J. Med.* **330**, 613 (1995); M. Memo, M. Pizzi, A. Valerio, M. Grilli, P. F. Spano, *Int. Rev. Psychiatry* **7**, 339 (1995).
2. P. L. McGeer and E. G. McGeer, *Brain Res. Rev.* **21**, 195 (1995).
3. P. Insel, in *Goodman and Gilman's The Pharmacological Basis of Therapeutics* J. G. Hardman, P. B. Molinoff, R. W. Rudden, A. Goodman Gilman, Eds. (McGraw-Hill, New York, 1996), pp. 617–657; K. D. Rainsford, in *Aspirin and the Salicylates* (Butterworths, London, 1984); G. Weismann, *Sci. Am.* **84**, 264 (January 1991); J. P. Famaey and H. E. Paulus, Eds., *Therapeutic Applications of NSAIDS Subpopulations and New Formulations* (Dekker, New York, 1992).
4. V. Gallo, M. T. Ciotti, F. Coletti, F. Aloisi, G. Levi, *Proc. Natl. Acad. Sci. U.S.A.* **79**, 7919 (1982); M. Favaron *et al.*, *ibid.* **85**, 7351 (1988).
5. Primary cultures of cerebellar granule cells were prepared from cerebella of 8-day-old rats (Sprague-Dawley) killed according to the Policy on the Use of Animals in Neuroscience Research. The cultures were used at 10 to 12 days in vitro and contained more than 95% glutamatergic neurons. Neurotoxicity was induced as described [M. Pizzi, C. Fallacara, V. Arrighi, M. Memo, P. F. Spano, *J. Neurochem.* **61**, 683 (1993)]. Drugs tested for neuroprotection were added 5 min before and during the glutamate pulse. Cell survival was evaluated 24 hours after the glutamate pulse as described by K. H. Jones and J. A. Senft [*J. Histochem. Cytochem.* **33**, 77 (1985)]. ASA, NaSal, and indomethacin did not affect neuronal viability per se.
6. M. Grilli, M. Pizzi, M. Memo, P. F. Spano, data not shown.
7. Hippocampal slices were obtained from brains of 8-day-old rats and prepared as described [G. Garthwaite and J. Garthwaite, *Neurosci. Lett.* **97**, 316 (1989)]. Slices were preincubated with either the test drugs, ASA and NaSal, or vehicle for 30 min, and then NMDA (30 μM) was added for an additional 30 min. Slices were washed and incubated in fresh buffer for 90 min and then fixed and embedded in epoxy resin. Semithin (1 μm) sections were cut, stained with methylene blue and azur II, and examined by light microscopy. For quantitation of cell loss, cells were counted in cell layer fields taken from CA1, CA3, and the dorsal blade of the DG in each slice. The fields measured 1.5×10^4 mm^2. The percentage of cell survival was calculated by the ratio of living cells to the total number of cells.
8. D. W. Choi, *J. Neurosci.* **7**, 369 (1987).
9. The $[Ca^{2+}]_i$ was measured by Fura-2 microfluorimetry in single cells as described by M. Pizzi *et al.* [*Mol. Pharmacol.* **49**, 586 (1996)]. Cells were exposed to glutamate for 2 min in Mg^{2+}-free Krebs-Ringer solution. ASA or NaSal was added 2 min before glutamate exposure. Fluorescence image acquisition and analysis were performed by using the MIRAcal (multiple image ratioing and analysis with calibration) system from Applied Imaging (England). Like ASA, NaSal (2 to 10 mM) produced a low and transient $[Ca^{2+}]_i$ increase without affecting glutamate-mediated calcium entry.
10. E. Kopp and S. Ghosh, *Science* **265**, 956 (1994).
11. H. C. Liou and D. Baltimore, *Curr. Opin. Cell Biol.* **5**, 477 (1993); M. Grilli, J.-S. Chiu, M. J. Lenardo, *Int. Rev. Cytol.* **143**, 1 (1993).
12. C. Kaltschmidt, B. Kaltschmidt, P. A. Baeuerle, *Mech. Dev.* **43**, 135 (1993); C. Kaltschmidt, B. Kaltschmidt, H. Neumann, H. Wekerle, P. A. Baeuerle, *Mol. Cell. Biol.* **14**, 3981 (1994); M. Grilli *et al.*, *J. Biol. Chem.* **270**, 26774 (1995); S. W. Barger and M. P. Mattson, *Mol. Brain Res.* **40**, 116 (1996)
13. C. Kaltschmidt, B. Kaltschmidt, P. A. Baeuerle, *Proc. Natl. Acad. Sci. U.S.A.* **92**, 9618 (1995); L. Guerrini, F. Blasi, S. Denis-Donini, *ibid.*, p. 9077; M. Grilli, F. Goffi, M. Memo, P. F. Spano, *J. Biol. Chem.* **271**, 15002 (1996).
14. T. Curran and B. R. Franza, *Cell* **55**, 395 (1988).
15. Nuclear extracts were prepared according to a small-scale protocol described by N. C. Andrews and D. V. Faller [*Nucleic Acids Res.* **19**, 2499 (1991)]. DNA binding reactions were performed as described [S.-M. Kang, A.-C. Tran, M. Grilli, M. J. Lenardo, *Science* **256**, 1452 (1992)] with the following modifications: 4 μg of nuclear extracts was combined with 50,000 cpm (0.2 ng) of γ-^{32}P–labeled oligonucleotides in a total volume of 12 μl. Oligonucleotide sequences were as follows: κB oligonucleotide sequence from the immunoglobulin κ light-chain gene, 5′-CAGAGGGGACTTTCCGAGAGGC-3′; AP-1 oligonucleotide sequence, 5′-CGCTTGATGAGTCAGCCGGAA-3′.
16. Indomethacin (1 to 20 μM) was tested for the ability to interfere with glutamate-induced NF-κB activation in cerebellar granule cells. No inhibition was observed. M. Grilli, M. Pizzi, M. Memo, P. F. Spano, unpublished material.

17. This work was partially supported by Consiglio Nazionale delle Ricerche, Italy.

26 June 1996; accepted 25 September 1996

Tricorn Protease—The Core of a Modular Proteolytic System

Tomohiro Tamura, Noriko Tamura, Zdenka Cejka, Reiner Hegerl, Friedrich Lottspeich, Wolfgang Baumeister*

Large macromolecular assemblies have evolved as a means of compartmentalizing reactions in organisms lacking membrane-bounded compartments. A tricorn-shaped protease was isolated from the archaeon *Thermoplasma* and was shown to form a multisubunit proteolytic complex. The 120-kilodalton monomer assembled to form a hexameric toroid that could assemble further into a capsid structure. Tricorn protease appeared to act as the core of a proteolytic system; when it interacted with several smaller proteins, it displayed multicatalytic activities.

In vivo proteolysis is an essential element of many regulatory processes. It must be subject to spatial and temporal control in order to prevent damage to the cell. Prokaryotic cells, which lack membrane-bounded compartments, have developed large macromolecular assemblies or "molecular organelles" so as to confine proteolysis to an inner cavity to which only proteins targeted for degradation have access. The paradigm of such a proteolytic complex is the proteasome (*1*), which is ubiquitous across the three urkingdoms archaea (*2*), bacteria (*3*, *4*) and eukarya (*5*). In the course of searching for regulatory components of the proteasome (*6*) in *Thermoplasma acidophilum*, we discovered a proteolytic complex of high molecular mass that is not related to the proteasome. This complex seems to be the core of a modular proteolytic system generating multicatalytic activities.

We purified the high-molecular-weight (HMW) protein to homogeneity by a sequence of chromatography steps (*7*). The purified protein migrates at 720 kD in gel filtration chromatography (versus migration at 680 kD by the 20S proteasome), and it turned out to be composed of a single polypeptide of 120 kD when subjected to SDS–polyacrylamide gel electrophoresis (SDS-PAGE) (Fig. 1). The purified protein

Max-Planck-Institute for Biochemistry, D-82152 Martinsried, Germany.

*To whom correspondence should be addressed.

was subjected to amino acid microsequence analysis. The gene encoding the 120-kD protein was cloned by means of inverse polymerase chain reaction (PCR) and PCR cloning methods (*8*). The cloned 5 kb of DNA encoded three open reading frames (ORFs). *orf1* encoded a protein homologous to a guanosine triphosphate–binding protein, *tri* encoded the 120-kD protein, and *orf2* encoded a previously unknown protein. The ORF of *tri* encoded 1071 amino acids with a calculated molecular weight of 121,635 daltons and an estimated isoelectric point of 5.8 (Fig. 2A).

The derived amino acid sequence of the 120-kD protein, which contained all of the internal sequences obtained by microsequencing, did not reveal any significant similarity with sequences of proteins in GenBank. In the COOH-terminal region (residues 878 to 1036), a weak but significant similarity to several COOH-terminal processing proteases (Ctp's) of bacterial and eukaryotic origin was observed (Fig. 2B). The near COOH-terminal regions of these proteases, in turn, have a homology of unknown functional significance to a sequence motif that is repeated four times in the interphotoreceptor retinol-binding protein (IRBP) of mammals (*9*). Among the bacterial Ctp's is the *Escherichia coli* tail-specific protease (Tsp), which was recently shown to degrade proteins translated from mRNAs without stop codons, using a COOH-terminally added sequence motif as a degradation signal (*10*). Of the residues that have been implicated in active site formation on the basis of mutational studies (*11*) in Tsp (Ser^{430}, Asp^{441}, and Lys^{445}), only the serine (Ser^{965}) is conserved in our 120-kD protein. This suggests that the COOH-terminal portion of our protein and the conserved region of the various Ctp's and of IRBP form a domain with a common fold, which may have a role in substrate binding.

In order to characterize the 720-kD complex further, we constructed a recombinant HMW (rHMW) protein, with an affinity tag coding for six consecutive histidine residues [$(His)_6$ tag] fused to the COOH-terminal end of the encoding gene; this allowed purification of the rHMW protein by Ni-NTA affinity chromatography and Mono-Q chromatography (*12*). The rHMW protein formed a homo-oligomeric complex that was indistinguishable from the 720-kD protein isolated from *Thermoplasma* cells in its ability to degrade fluorogenic peptides (Table 1) and casein (*13*). Unlike the 20S proteasome from *T. acidophilum*, which cleaves chymotrypsin-like substrates, the rHMW protease preferentially cleaved trypsin-like substrates. However,

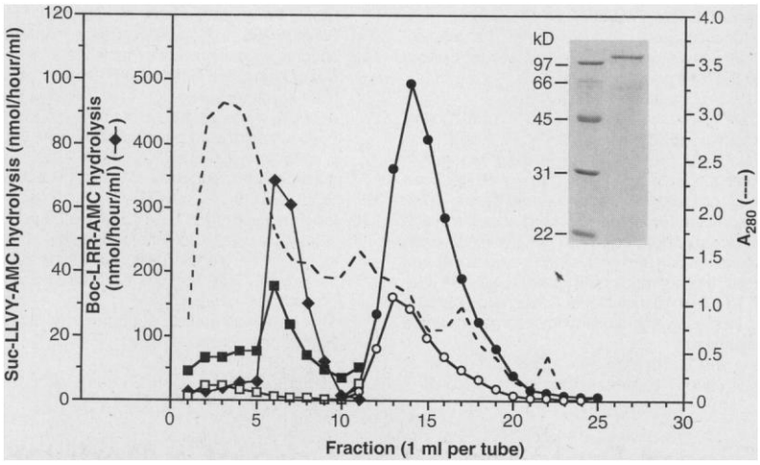

Fig. 1. Isolation of TRI and two different factors from *T. acidophilum*. Suc-LLVY-AMC cleaving activity in a glycerol density gradient (GDG) fraction is shown. Crude extract from *T. acidophilum* (6.5 mg) was fractionated by 10 to 40% GDG into 1-ml fractions. Activity was tested by incubation of 20 μl (○) (corresponding to proteasome activity) or 50 μl (□) of each fraction with 10 nmol of peptide for 1 hour at 60°C. In addition, 50 μl of pooled LMW fractions (fractions 6 and 7) was incubated with 20 μl of HMW fractions (●) (mostly TRI-enhanced activity), and 20 μl of pooled TRI-containing fractions (fractions 17 and 18) was incubated with 50 μl of LMW fractions (■) for 1 hour at 60°C. The Boc-LRR-AMC-enhanced hydrolyzing activity was teasted by incubation of 10 μl of GDG fractions with 0.4 μg of rTRI. Data were plotted as enhanced peptidase activities (◆). The inset shows SDS-PAGE of the purified TRI proteins.

Fig. 2. Genetic and primary structure of TRI (*17*). (**A**) The deduced amino acid sequence of TRI. Peptide sequences that were obtained by Edman degradation are underlined, and sequences for which synthetic oligonucleotides were constructed are indicated by double underlines. The sequence has been submitted to GenBank (accession number U72850). (**B**) Schematic alignment of TRI from *T. acidophilum* (Ta), human interphotoreceptor retinol-binding protein (hIRBP), and Ctp homologs from eubacteria (Ec, *E. coli*; Hi, *Haemophilus influenzae*; Bb, *Bartonella bacilliformis*; Sy, *Synechocystis sp.* PCC 6803; and Aq, *Agmenellum quadruplicatum*) and a eukaryote (Sp, *Spinach*). Shaded boxes indicate the regions of homology with the IRBP domain.

A

```
MPSLMSFGSCQWIDQGRFSRSLYRNFKTFKLHEMHGLCMPNLLLNPDIHGDRIIFVCCDDLWEHDLKSGSTRKIVSNLGVINNARFFPDGRKIAIRVMRG  100
SSLNTADLYFYNGENGEIKRITYFSGKSTGRRMFTDVAGFDPDGNLIISTDAMQPFSSMTCLYRVENDGINFVPLNLGPATHILFADGRRVIGRNTFELP  200
HWKGYRGGTRGKIWIEVNSGAFKKIVDMSTHVSSPVIVGHRIYFITDIDGFGQIYSTDLDGKDLRKHTSFTDYYPRHLNTDGRRILFSKGGSIYIFNPDT  300
EKIEKIEIGDLESPEDRIISIPSKFAEDFSPLDGDLIAFVSRGQAFIQDVSGTYVLKVPEPLRIRYVRRGGDTKVAFIHGTREGDFLGIYDYRTGKAEKF  400
EENLGNVFAMGVDRNGKFAVVANDRFEIMTVDLETGKPTVIERSREAMITDFTISDNSRFIAYGFPLKHGETDGYVMQAIHVYDMEGRKIFAATTENSHD  500
YAPAFDADSKNLYYLSYRSLDPSPDRVVLNFSFEVVSKPFVIPLIPGSPNPTKLVPRSMTSEAGEYDLNDMYKRSSPINVDPGDYRMIIPLESSILIYSV  600
PVHGEFAAYYQGAPEKGVLLKYDVKTRKVTEVKNNLTDLRLSADRKTVMVRKDDGKIYTFPLEKPEDERTVETDKRPLVSSIHEEFLQMYDEAWKLARDN  700
YWNEAVAKEISERIYEKYRNLVPLCKTRYDLSNVIVEMQGEYRTSHSYEMGGTFTDKDPFRSGRIACDFKLDGDHYVVAKAYAGDYSNEGEKSPIFEYGI  800
DPTGYLIEDIDGETVGAGSNIYRVLSEKAGTSARIRLSGKGGDKRDLMIDILDDDRFIRYRSWVEANRRYVHERSKGTIGYIHIPDMGMMGLNEFYRLFI  900
NESSYQGLIVDVRFNGGGFVSQLIIEKLMNKRIGYDNPRRGTLSPYPTNSVRGKIIAITNEYAGSDGDIFSFSFKKLGLGKLIGTRTWGGVVGITPKRRL 1000
IDGTVLTQPEFAFWFRDAGFGVENYGVDPDVEIEYAPHDYLSGKDPQIDYAIDALIEELRNWNEELPQRPS                                1071
```

B

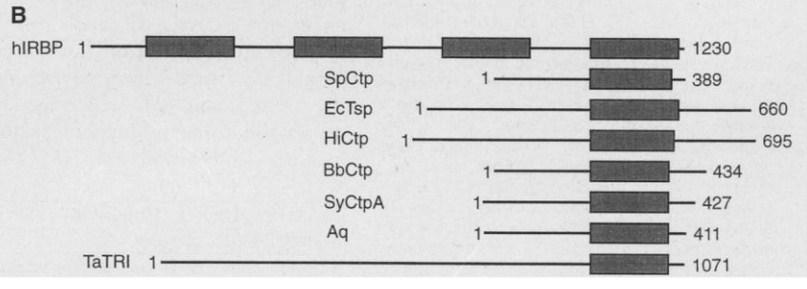

one chymotrypsin-like substrate, alanyl-alanyl-phenylalanyl-7-amino-4-methylcoumarin (H-AAF-AMC), was also cleaved; when this peptide carried a negative charge at the NH_2-terminal end (Suc-AAF-AMC), it was not cleaved (Table 1). Inhibitor experiments using a variety of compounds showed that the peptidase activity of the complex was efficiently inhibited only by tosyl-L-phenylalanine chloromethyl ketone (TPCK) (median inhibitory concentration = 40 μM) or by tosyl-L-lysine chloromethyl ketone (TLCK), which indicates that a histidine residue may be involved in active site formation. In these assays, the proteolytic activity of the rHMW was independent of adenosine triphosphate (ATP)–Mg^{++}. The optimum temperature (~ 65°C) was slightly above the growth temperature of *T. acidophilum*; the optimum pH was between 8.5 and 8.8.

We examined preparations of the 720-kD protease isolated from *T. acidophilum*, as well as the recombinant protein, by electron microscopy in conjunction with image analysis techniques (Fig. 3, A through E). The preparations were indistinguishable from each other and showed the HMW complex in a variety of different orientations. Most conspicuous was a tricorn-shaped motif ["tricorne" is French and means "chapeau à bords repliès en trois cornes"], approximately 18 nm in diameter and with a prominent stain-filled center. We refer to this projection down the threefold symmetry axis as the end-on view and hereafter call this protein the tricorn protease (TRI). A projection with twofold symmetry, a width corresponding to the diameter of the end-on view, and a height of approximately 10 nm was also frequently found (the side-on view) (Fig. 3B). Orientations intermediate between these two were also observed and were exploited in performing a three-dimensional reconstruction with the use of a method closely akin to angular reconstitution (*14*) (Fig. 3, B, D, and E).

Although there is no detectable sequence similarity and the dimensions are different, the TRI bears a striking resemblance to the Gal6 or bleomycin hydrolase from *Saccharomyces cerevisiae*, a protease that binds to DNA (*15*). We have no evidence that TRI has a DNA binding ability. Both molecules are built from six identical subunits arranged with 32-point group symmetry, forming a toroidal structure traversed by a channel along the threefold-axis. Inside the hexamer, the channel widens into a cavity that is approximately 8 nm in diameter in TRI protease, which is much wider than the analogous cavities in the Gal6 or bleomycine hydrolase (4.5 nm) or the *Thermoplasma* proteasome (5.3 nm).

During the last purification step (chromatography on a Superose 6 column), the concentrated TRI showed a tendency to fractionate into the void volume and into the 720-kD fraction. Electrophoretic analysis of both fractions revealed a single 120-kD band, and the two fractions were equiv-

Table 1. Hydrolysis of synthetic substrates by native or recombinant tricorn protease and the proteasome from *T. acidophilum*. Activity was assayed by incubation of 0.32 μg of purified tricorn protease, 0.416 μg of recombinant tricorn protease, or 0.28 μg of purified proteasome with 10 nmol of fluorogenic substrates (final concentration, 100 μM; purchased from Bachem) for 60 min at 60°C . The fluorescence of AMC was measured. Z, benzoxycarbonyl; Bz, benzoyl.

	Tricorn protease (nmol $hour^{-1}$ mg^{-1})		Proteasome (nmol $hour^{-1}$ mg^{-1})
	Native	Recombinant	
	Trypsin-like activity		
Z-Gly-Gly-Arg-AMC	138	209	0
Boc-Leu-Arg-Arg-AMC	347	389	0
Z-Ala-Arg-Arg-AMC	334	308	0
Bz-Val-Gly-Arg-AMC	997	1257	0
	Chymotrypsin-like activity		
Suc-Leu-Tyr-AMC	0	0	0
Suc-Ala-Ala-Phe-AMC	0	0	400
H-Ala-Ala-Phe-AMC	5125	6460	978
Suc-Leu-Leu-Val-Tyr-AMC	0	0	1432
Z-Gly-Gly-Leu-AMC	0	0	1750

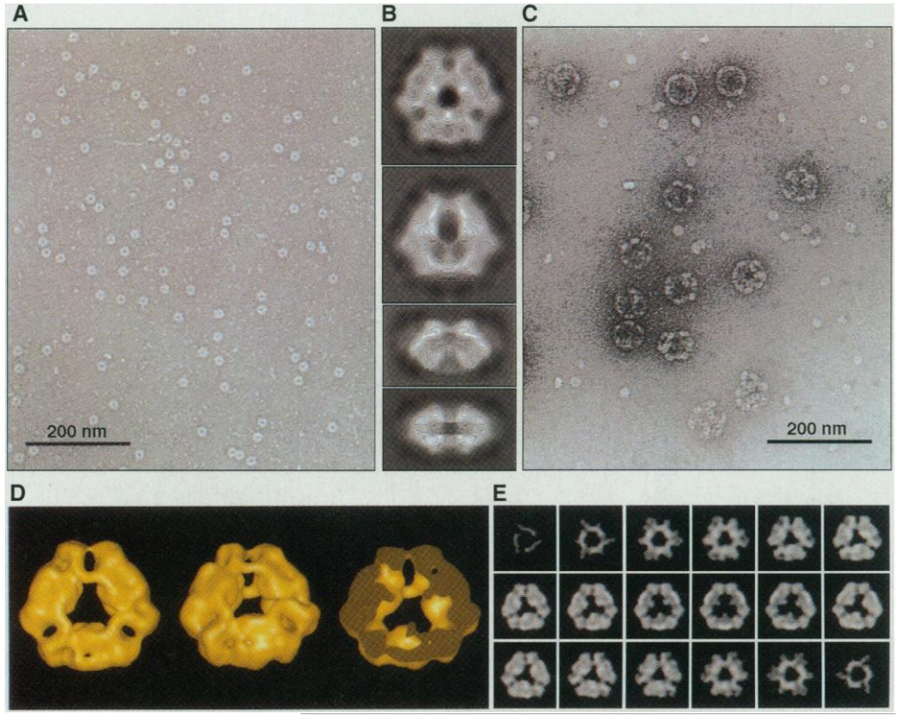

Fig. 3. Electron microscopic characterization of TRI from *T. acidophilum*. The fraction is from Superose 6 chromatography; the 720-kD fraction as well as the void volume fractions were subjected to electron microscopy. (**A**) Characteristic appearance of the 720-kD fraction, showing the TRI complex predominantly in end-on orientation. (**B**) Gallery of averages ranging from end-on (top) to side-on orientation (bottom). (**C**) Characteristic appearance of the void volume fraction, showing numerous completely or partially assembled capsids. (**D**) Three-dimensional reconstruction of TRI with 32-point group symmetry imposed. This is a shaded isosurface representation viewed along the threefold axis of the molecule. Three twofold axes are in the plane perpendicular to the threefold axis (left). The view was obtained by tilting the model around an axis that is in the plane of the twofold axes and perpendicular to one of them (center). The same view but with the upper half of the molecule removed is shown at right. (**E**) Gallery of sections perpendicular to the threefold axis. The distance between two neighboring sections corresponds to a pixel size of 0.5 nm.

alent in terms of their peptidase activity. When the void volume fraction was examined by electron microscopy, we found numerous isometric capsid structures, approximately 54 nm diameter, that were assembled from the TRI toroids (Fig. 3C). We have no information about whether these capsids have any physiological importance.

When we mixed TRI with fractions of low molecular weight (LMW), several different peptidase activities were generated or enhanced: succinyl-leucyl-leucyl-valyl-tyrosyl-AMC (Suc-LLVY-AMC) and *N*-*t*-butoxycarbonyl-leucyl-arginyl-arginyl-AMC (Boc-LRR-AMC) (Fig. 1). We referred to these activating factors as F1 (LLVY) and F2 (LRR), respectively. The factors were purified from *T. acidophilum* cell extracts and characterized. F1 was found to be a 34-kD protein with significant homology to eubacterial proline iminopeptidases (PIPs) and was shown to have PIP activity when substrates such as H-Pro-AMC were used (*16*). We obtained preliminary evidence that F2 may also be an amino-peptidase (*13*).

Purified F1 and partially purified F2 alone showed H-AAF-AMC cleaving activity. When the TRI-dependent peptidase activities were tested in reconstitution experiments with a variety of fluorogenic peptides (Fig. 4), activities were generated that neither TRI nor these activating factors alone possessed: TRI plus F1 or F2 yielded Suc-LLVY-AMC hydrolyzing activity. Moreover, these factors and TRI cooperatively enhanced their intrinsic peptidase activities: F1 plus TRI enhanced the H-AAF-AMC hydrolyzing activity, and F2 plus TRI enhanced the Boc-LRR-AMC hydrolyzing activity. A detailed biochemical characterization of F1 will be reported elsewhere (*16*).

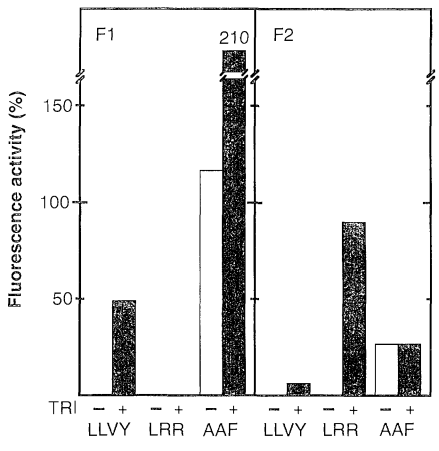

Fig. 4. LMW factors and TRI jointly generate novel peptidase activities. Recombinant PIP (1 μg) and partially purified F2 protein (0.11 μg) were incubated with 10 nmol of fluorogenic (AMC) substrate for 15 min at 60°C in the presence or absence of rTRI (0.7 μg). The fluorescence of released AMC was measured after the reaction was stopped. The indicated activities show the enhancement of peptidase activities of F1 and F2 provided by TRI. One hundred percent fluorescence activity corresponds to 2 nmol of released AMC.

TRI, F1, and F2 appear to be components of a modular proteolytic system, which could generate multicatalytic peptidase activities by interacting with each other. These interactions enhanced the intrinsic activities of the components but could also generate new types of peptide-hydrolyzing activities. The precise mode of the interactions between TRI and the two factors, as well as their role in regulated proteolytic events in vivo, remain to be elucidated.

REFERENCES AND NOTES

1. J. Löwe *et al.*, *Science* **268**, 533 (1995); E. Seemüller *et al.*, *ibid.*, p. 579; G. Pühler *et al.*, *EMBO J.* **11**, 1607 (1992); T. Wenzel and W. Baumeister, *Nature Struct. Biol.* **2**, 199 (1995); A. Lupas, A. J. Koster, W. Baumeister, *Enzyme Protein* **47**, 252 (1993); D. M. Rubin and D. Finley, *Curr. Biol.* **5**, 854 (1995).
2. B. Dahlmann *et al. FEBS Lett.* **251**, 125 (1989); J. A. Maupin-Furlow and J. G. Ferry, *J. Biol. Chem.* **270**, 28617 (1995).
3. A. Lupas, P. Zwickl, W. Baumeister, *Trends Biochem. Sci.* **19**, 533 (1994).
4. T. Tamura *et al.*, *Curr. Biol.* **5**, 766 (1995).
5. M. Orlowski, *Biochemistry* **29**, 10289 (1990); K. Tanaka, T. Tamura, T. Yoshimura, A. Ichihara, *New Biol.* **4**, 173 (1992); A. J. Rivett, *Biochem. J.* **291**, 1 (1993).
6. O. Coux, K. Tanaka, A. L. Goldberg, *Annu. Rev. Biochem.* **65**, 801 (1996).
7. *Thermoplasma acidophilum* cells (ATCC 25905) were grown at 58°C at pH 1.0 [C. Christiansen, E. A. Freundt, F. T. Black, *Int. J. Sys. Bacteriol.* **25**, 99 (1975)]. Cultured cells were harvested and resuspended in 5 volumes of homogenate buffer [100 mM Hepes (pH 8.0), 1 mM dithiothreitol (DTT), 5 mM $MgCl_2$, 5 mM ATP, and DNaseII (10 μg/ml)] and incubated for 30 min at room temperature before lysis by sonication. The lysate was centrifuged for 1 hour at 61,700*g*. Glycerol was added to the supernatant (the final 20%), which was stored at −80°C until use. Throughout the purification procedures for TRI and F1 protein, peptidase activity was tested by addition of either pooled LMW fractions or pooled HMW fractions, which were fractionated by a 10 to 40% glycerol density gradient by means of centrifugation at 25,000 rpm for 22 hours at 4°C with a SW28 rotor (Beckman). For the F2 protein purification, the peptidase activities were tested by addition of recombinant TRI (rTRI). Peptidase assays were performed in 100 μl of 50 mM tris-HCl (pH 8.0), and released AMC was measured as previously described (*4*). For isolation of TRI, 2.8 g of lysate from *T. acidophilum* cells were used for purification. The purified protein (900 μg) was dialyzed against 50 mM tris-HCl (pH 7.5) with 20% glycerol and stored at 4°C. For isolation of the F1 protein, 900 mg of lysate from *T. acidophilum* cells was subjected to the purification procedure. The purified protein (40 μg) was dialyzed with 25 mM tris-HCl buffer (pH 7.5) containing 1 mM DTT, and was stored at 4°C. For isolation of F2, 1.36 g of lysate from *T. acidophilum* cells were used for purification. Partially purified F2 (390 μg) was dialyzed with 50 mM tris-HCl buffer (pH 7.5) and stored at 4°C. Purified TRI and the F1 protein were subjected to amino acid sequence analysis. A detailed description of the purification procedure is available on request (e-mail: tamura@vms.biochem.mpg.de).
8. *Thermoplasma acidophilum* chromosomal DNA was purified by phenol-chloroform extraction. PCR was carried out with 8- to 16-fold degenerated primers that were designed from the peptide sequences as indicated in Fig. 2A. Pair 1 was AT[A/T]TATAT[A/T] TTTAATCC [G/T]GATAC[G/T]GA and GC[G/T]AC[G/T] GCTTCGT-TCCAGTAGTT[A/G]TC. Pair 2 was GAGAAT[A/T][G/C] TCATGATTATGC[G/T]CC[G/T]GC and GC[G/T]AC[G/T]GCTTCGTTCCAGTAGTT[A/G]TC. Pair 1 primers gave rise to a 1244–base pair (bp) fragment and pair 2 primers produced a 635-bp fragment. The fragments were isolated and sequenced, and then specific primers were redesigned for use in either inverse PCR [H. Ochman, M. M. Medhora, D. Garza, D. L. Hartl, in *PCR Protocols: A Guide to Methods and Applications*, M. A. Innis, D. H. Gelfand, J. J. Sninsky, T. J. White, Eds. (Academic Press, San Diego, CA, 1990), pp. 219–227] or PCR screening [D. Alfandari and T. Darribère, *PCR Methods Appl.* **4**, 46 (1994)]. With PCR screening, we constructed a gene library in pBluescript IISK(+) that carried 3 to 6 kb of *T. acidophilum* chromosomal DNA, partially digested by Sau 3AI. The library was transformed to XL-1 blue cells. A total of 7200 transformants was screened and one positive clone was obtained: the purified plasmid carrying the NH_2-terminal truncated TRI-encoding gene. To obtain the missing region, chromosomal DNA was digested by Ava I or Ban II, circularized with T4 ligase, and subjected to inverse PCR. The amplified 1317-bp and 2079-bp fragments were purified and subjected to sequence analyses. The cloned ORF encoding the 120-kD protein has two possible initiation codons, Met1 and Met5; and a putative ribosomal binding site, which is found downstream of the initiation codon in archaea [W. Zillig *et al.*, *Eur. J. Biochem.* **173**, 473 (1988)], is located between both methionines. We tentatively selected Met1 as the initiation codon because it encodes the longest ORF.
9. G. I. H. Liou, L. Geng, W. Baehr, in *The Molecular Biology of the Retina: Basic and Clinically Relevant Studies*, D. B. Farber and G. J. Chader, Eds. (Wiley-Liss, New York, 1991), pp. 115–137.
10. S. Jentsch, *Science* **271**, 955 (1996); K. C. Keiler, P. R. H. Waller, R. T. Sauer, *ibid.*, p. 990.
11. K. C. Keiler and R. T. Sauer, *J. Biol. Chem.* **270**, 28864 (1995).
12. The TRI-encoding gene was amplified as two overlapped segments: an NH_2-terminal and a COOH-terminal encoding fragments by PCR using four oligonucleotides: (i) with a flanking Nde I-site; (ii) with an Eco RI-site downstream of the TRI encoding gene; (iii) with an Eco RI-site found upstream of the TRI encoding gene; and (iv) with a $(His)_6$ tag and a flanking Xho I site. The amplified NH_2 terminally encoded fragment was digested with Nde I and Eco RI and cloned into the same sites of a pT7-7 expression vector [S. Tabor and C. C. Richardson, *Proc. Natl. Acad. Sci. U.S.A.* **82**, 1074 (1985)], yielding a pT7-7(N). The other half of the fragment was digested with Eco RI and Xho I and cloned into the Eco RI and Sal I sites of pT7-7(N), yielding a pT7-7(TRI). The $(His)_6$-tagged TRI was expressed in *E. coli* BL21(DE3) cells [F. W. Studier, A. H. Rosenberg, J. J. Dunn, J. W. Dubendorff, *Methods Enzymol.* **185**, 60 (1990)] containing a pUBS520 plasmid encoding the *dnaY* gene [U. Brinkmann, R. E. Mattes, P. Buckel, *Gene* **85**, 109 (1989)]. The recombinant proteins were purified on a Ni-NTA resin (Diagen, Hilden, Germany) and a Mono-Q column and dialyzed against 50 mM tris-HCl (pH 7.5) with 20% glycerol. The expression level of rTRI in pUBS520-transformed BL21 cells was 10 times higher than in normal BL21 cells. The structure of recombinant protein was confirmed by electron microscopy.
13. T. Tamura, N. Tamura, W. Baumeister, unpublished results.
14. Protein was negatively stained with uranyl acetate. The conditions of image recording and image analysis were as detailed [W. Baumeister *et al.*, *FEBS Lett.* **241**, 239 (1988)]. Due to the occurrence of the molecule in different orientations, the reconstruction was performed with a procedure for a posteriori determination of relative projection directions. The approach is based on sinogram correlation [M. van Heel, *Ultramicroscopy* **21**, 111 (1987)] in conjunction with an optimum alignment approach that is similar to a method described previously [N. A. Farrow and F. P. Ottensmeyer, *J. Opt. Soc. Am.* **A9**, 1749 (1992)]. A

weighted back-projection was used to calculate the three-dimensional density map. The alignment was carried out with four projection views obtained by eigenvector-eigenvalue classification and averaging (see also Fig. 3B). Although these projections are not related by symmetry, further projections were incorporated by imposing 32-point group symmetry. A reconstruction imposing threefold symmetry only was virtually identical to the reconstruction using the full 32-point group symmetry, which indicates that the preparation does not suffer from significant preparation-induced distortions. For the isosurface representation, a threshold value was chosen that relates the volume of the model to a molecular weight of 730-kD if a density of 1.3 g cm^{-3} is assumed.

15. L. Joshua-Tor, H. E. Xu, S. A. Johnston, D. C. Rees, *Science* **269**, 945 (1995).
16. T. Tamura, N. Tamura, F. Lottspeich, W. Baumeister, *FEBS Lett.*, in press.
17. Single-letter abbreviations for the amino acid residues are as follows: A, Ala; C, Cys; D, Asp; E, Glu; F, Phe; G, Gly; H, His; I, Ile; K, Lys; L, Leu; M, Met; N, Asn; P, Pro; Q, Gln; R, Arg; S, Ser; T, Thr; V, Val; W, Trp; and Y, Tyr.
18. We thank R. M. Glaeser (University of California, Berkeley), A. Lupas, and M. A. Kania for critically reading the manuscript; M. Boicu for DNA sequencing; and R. Mattes (University of Stuttgart) for providing the *dnaY* gene. T.T. acknowledges a Postdoctoral Fellowship for Research Abroad from the Japan Society for the Promotion of Science. This work was also supported by a grant from the Human Frontier Science Program to W.B.

14 August 1996; accepted 18 October 1996

Control of *C. elegans* Larval Development by Neuronal Expression of a TGF-β Homolog

Peifeng Ren,* Chang-Su Lim,*† Robert Johnsen,‡
Patrice S. Albert, David Pilgrim, Donald L. Riddle§

The *Caenorhabditis elegans* dauer larva is specialized for dispersal without growth and is formed under conditions of overcrowding and limited food. The *daf-7* gene, required for transducing environmental cues that support continuous development with plentiful food, encodes a transforming growth factor–β (TGF-β) superfamily member. A *daf-7* reporter construct is expressed in the ASI chemosensory neurons. Dauer-inducing pheromone inhibits *daf-7* expression and promotes dauer formation, whereas food reactivates *daf-7* expression and promotes recovery from the dauer state. When the food/pheromone ratio is high, the level of *daf-7* mRNA peaks during the L1 larval stage, when commitment to non-dauer development is made.

The soil nematode *C. elegans* develops to adulthood through four larval stages (L1 through L4) with abundant food, but as population density increases and bacterial food supply diminishes, the nonfeeding dauer larva may be formed at the second molt (*1*). Entry into, and exit from, the dauer stage are influenced by temperature, food supply, and a *Caenorhabditis*-specific dauer-inducing pheromone, the concentration of which reflects population density (*2*, *3*). Mutations in *daf-7* result in constitutive dauer larva formation even with abundant food (*4*). Killing amphid chemosensory neurons ASI, ADF, ASG, and ASJ with a laser microbeam results in a dauer-constitutive phenocopy at 20°C (*5*). Molecular evidence reported here suggests that DAF-7 acts as a negative regulator of dauer larva development by transducing chemosensory information from ASI neurons.

Using Tc1 transposon tagging (*6*) and DNA transformation rescue (*7*), we cloned the *daf-7* gene (*8*) (Fig. 1A). The predicted gene product contains the conserved characteristics of the TGF-β superfamily (*9*) (Fig. 1B). Within the ligand domain, *daf-7* contains the seven cysteines nearly invariant in the superfamily, and it has two additional cysteines previously found only in the vertebrate homologs TGF-β and activin. Comparisons of the ligand domain show that DAF-7 has 34% amino acid sequence identity with human bone morphogenetic protein–4 (BMP-4), 34% with *Drosophila decapentaplegic* (*dpp*) protein, and 28% with human TGF-β, but lacks several amino acids invariant in these subfamilies. Hence, it is a new subtype of the TGF-β superfamily.

We sequenced *daf-7* mutant alleles (*10*) (Fig. 1B) and measured the severity of the temperature-sensitive (ts) dauer-constitutive (Daf-c) mutant phenotypes (*4*) (Table 1). The Tc1 transposon insertion strain (*m434::Tc1*) has residual *daf-7* activity, possibly due to removal of Tc1 during mRNA processing (*11*). Among six ethylmethane sulfonate–induced mutations, *m62* and *m88* are nonsense mutations suppressible by the *sup-7* amber suppressor (*12*), and *m83* generates a UGA codon in the pro-domain. Although these three mutant strains should produce truncated DAF-7 lacking most of the ligand domain and presumably are null mutants, they still exhibit a ts Daf-c phenotype

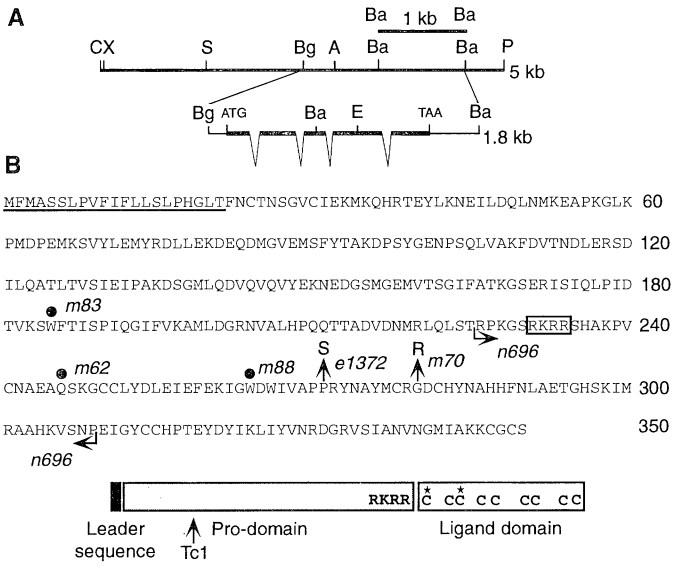

Fig. 1. *daf-7* encodes a TGF-β superfamily member. (**A**) Restriction map of a 5-kb genomic fragment that efficiently rescues *daf-7* mutants. Shown below is the intron-exon structure. C, Cla I; X, Xba I; S, Sal I; Bg, Bgl II; A, Acc I; Ba, Bam HI; E, Eco RI; P, Pst I. (**B**) Amino acid sequence of precursor protein beginning with the first predicted methionine, with leader sequence (underlined) and proteolytic cleavage site, RKRR (boxed). Mutation sites are indicated by arrows or dots. Shown below is a schematic of the *daf-7* protein indicating conserved TGF-β superfamily features and the point of Tc1 insertion. Two of the conserved cysteines (asterisks) in the ligand domain are found only in TGF-β and activin. GenBank accession numbers: U72883 for cDNA and U72884 for genomic DNA. Abbreviations for the amino acid residues are as follows: A, Ala; C, Cys; D, Asp; E, Glu; F, Phe; G, Gly; H, His; I, Ile; K, Lys; L, Leu; M, Met; N, Asn; P, Pro; Q, Gln; R, Arg; S, Ser; T, Thr; V, Val; W, Trp; and Y, Tyr.

P. Ren, C.-S. Lim, R. Johnsen, P. S. Albert, D. L. Riddle, Molecular Biology Program and Division of Biological Sciences, 311 Tucker Hall, University of Missouri, Columbia, MO 65211, USA.
D. Pilgrim, Department of Biological Sciences, G-507 Biological Sciences Building, University of Alberta, Edmonton, Alberta, Canada T6G 2E9.

*These authors contributed equally to this work.
†Present address: Department of Microbiology, Chungbuk National University, Cheongju, Chungbuk 360-763, Korea.
‡Present address: Department of Medical Genetics, University of British Columbia, 6174 University Boulevard, Vancouver, British Columbia, Canada V6T 1Z3.
§To whom correspondence should be addressed. E-mail: riddle@biosci.mbp.missouri.edu